The evaluation of photo/e-beam complementary grayscale lithography for high topography 3D structure

Liya Yu, Richard J. Kasica, Robert N. Newby, Lei Chen, Vincent K. Luciani
Center for Nanoscale Science and Technology, National Institute of Standards and Technology,
100 Bureau Drive, Gaithersburg, MD, USA 20899

ABSTRACT

This article demonstrates and evaluates photo/e-beam grayscale complementary lithography processes for the fabrication of large area, high topography grayscale structure. The combination of these two techniques capitalizes on the capability of photolithography to generate large three-dimensional structures and the ability of e-beam lithography to add fine structure while maintaining high vertical resolution. The litho-etching-litho-etching process reduces the challenges associated with the etching process when transferring fine features simultaneously with deep substrate etching. As a result, this approach enables the fabrication of large-scale high topography features with fine detail. In the first lithography step, a large staircase is fabricated by direct write photolithography. After the photolithography pattern has been transferred into the substrate, e-beam resist is deposited on the patterned substrate using spray coating to obtain conformal coverage on the deep stepped structure. In the second exposure step, an e-beam system further patterns the steps with finer features. Only a small number of grayscale levels are exposed which simplifies the required proximity correction in the design. A vertical resolution of 25 ± 5 nm in a 600 nm horizontal dimension and 45 ± 6 nm in a 300 nm horizontal feature are achieved over a 2 μm to 30 μm vertical depth range. The process, alignment strategy, overlay error, and process optimization of integrating high topography and grayscale structure are discussed.

Keywords: 3D structure, grayscale, complementary lithography, mix and match, e-beam, direct write, spray coating, high topography

1. INTRODUCTION

The fabrication of 3D microstructures is important to many applications including diffractive optics, photonic elements, micro-electromechanical systems, and micro-fluidic devices. The possible methods of fabrication used to overcome the 2D limitation of traditional lithography include mechanical, optical, electron-beam lithography, and X-ray lithography. Grayscale lithography is a technique that modulates the local energy dose exposing the resist so that a 3D structure is produced during the development step. The relationship between clearance depth d (cm) and the energy E (mJ/cm^2) could be expressed as:

$$d = A + B\log(E) \tag{1}$$

where

$$A = (1/\alpha)\ln(\alpha(1-R)/W_0) \tag{2}$$

$$B = 2.303/\alpha \tag{3}$$

Here α is absorption coefficient (cm^{-1}), R is reflectivity and W_0 is the energy absorbed per cm^3 at clearance depth d (cm). The absorption coefficient can be determined from the Dill parameters of the photoresist. The photoresist is fully exposed when the dose is greater than the dose-to-clear energy. Accurate 3D shaping of the upper surface of the photoresist with tight process control is the key to this technique. Proper control of the energy and developing process facilitates the generation of a continuous gradient or discrete stepped profile in photoresist, and subsequently in silicon, after reactive ion etching (RIE) or other dry etching techniques. In recent years, interest has accelerated in the development of methods for fabricating of 3D structures due to the increasing applications in micro- and nano-scale device fields.

1.1 Direct write grayscale lithography

Grayscale photolithography using grayscale masking is the most mature grayscale technique among all established techniques. It is possible to create grayscale photo-masks that can be used in a conventional mask aligner and projection photolithography tool by using sub-wavelength dithering (pixilated mask)[1], e-beam exposure of a high-energy-beam-sensitive glass,[2] dyed polymers of varying thickness, or laser-induced oxidation of metallic films.[3] However, most grayscale masks are expensive to fabricate, making them less attractive for applications in which frequent revisions may be necessary or only small quantities are required. An alternative method of varying the photoresist dose is to directly write the image using a laser pattern generator such as a laser writer. The grayscale principle has also been successfully used in the e-beam lithography in the past to produce devices such as high-efficiency gratings.[4] The combination of precise dose control, high resolution, and low surface roughness makes e-beam lithography an attractive choice for grayscale lithography in the sub-micron regime. Although the associated long write times make the direct write technique less attractive for manufacturing, it is more flexible in terms of generating an arbitrary profile and pattern revision.

1.2 Complementary gray scale lithography

Complementary Lithography was introduced by Yan Borodovsky in 2010[5] to take advantage of the best of both photolithography and e-beam lithography (EBL) to pattern next generation semiconductors. Logic and SOC (System-on-Chip) devices are going beyond a 20 nm half-pitch; however, device designers are moving toward a new 1D layout style. Optical lithography offers the most mature and cost-effective solution to pattern unidirectional, interference-like parallel lines; EBL is used to pattern critical layers including line cuts, via holes and contact holes at advanced technology nodes.[6] In addition to the advantage of processing efficiency, it also permits the ability to choose the best lithography technology for each step since each of these steps is separate and discreet.

As medical and optical device designers are shifting structures toward smaller and deeper dimensions without reducing the total device area, a similar mix and match approach seems prudent to fulfill this new trend of 3D device design practically in the future. Grayscale photolithography provides a high throughput and large area 3D structure fabrication but there is a resolution limit on the minimum pixel size due to the exposure wavelength, which sets the upper limit for the features and spacing. Resist behavior is also further complicated by surface inhibition effects and standing wave interactions with the substrate. E-beam lithography possess the advantage of fine vertical and horizontal step resolution but the limitation of resist options, proximity effect and low throughput limit the range of etching depth and device area. Therefore, the aims of this paper are to demonstrate this newly proposed concept of complementary grayscale lithography to generate a deep 3D structure with fine grayscale step as illustrated in Figure 1 and evaluate the possible challenges of realizing this new concept. In this paper, we also present for the first time spray coating of e-beam resist for grayscale lithography and investigate the film quality. The processing steps, results, and challenges of integrating the high topography with grayscale structures via direct write photolithography and e-beam lithography are discussed in this paper.

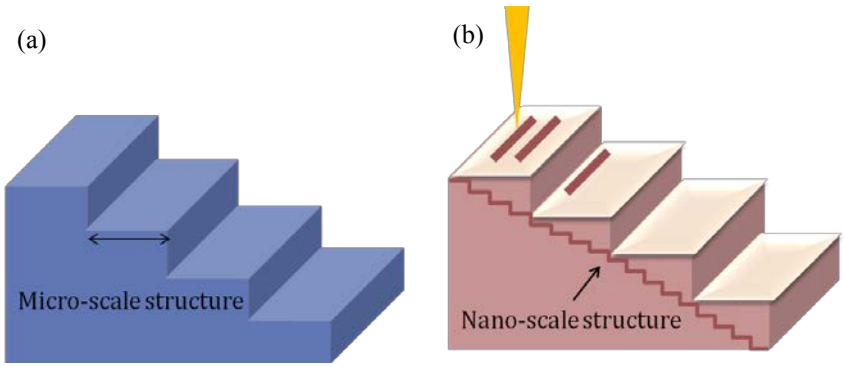

Figure 1. Two main steps of fabricating a high topography grayscale structure which is used in this paper to demonstrate the capability of complementary grayscale lithography.

2. PROCESS OPTIMIZATION AND RESULTS

Our aim is to generate fine grayscale features on high topography substrate structure via direct write photolithography and e-beam lithography. The first lithography is direct write photolithography. It was used to generate grayscale stairway pattern in micro-scale all over the 100 mm wafer with large device area. After the patterns were transferred into 2 μm and 30 μm deep substrates by dry etching, e-beam resist was spin-coated on 2 μm deep substrate and spray-coated on 30 μm substrate. With the proper cross-tool alignment design, e-beam lithography was implemented as second lithography to sculpture the fine steps with a sparse but high-resolution pattern. All the experimental work was performed in NIST NanoFab at Center of Nanoscale Science and Technology (CNST).

2.1 Grayscale photolithography

The direct write photolithography was performed using a laser pattern generator with 405 nm wavelength laser source at 110 mW output power. The exposure mode of the laser writer is binary and the writing intensity is assigned by percentage. With proper pattern fracturing, different intensities were assigned to different segments in the job writing and the binary exposure mode could function as grayscale exposure within the limited grayscale level. Three types of commercially available broad band / i-line photoresist listed in Table 1 are evaluated based on 6 μm and 8 μm wide staircase patterns. The film thickness was measured via reflectometry with a 10 nm tolerance.

Table 1. Resist properties of three types of broad band / i-line photoresists evaluated by direct write grayscale. The thickness listed in the table is the nominal thickness using spin speed 4000 min^{-1}.

Type	Thickness (μm)	Resolution (nm)
A	≈0.8	≈200
B	≈1.0	≈400
C	≈1.3	≈700

Type A and C both show good reproducibility of grayscale patterns. Type C shows a fairly stable performance over a large range of focus depth as indicated by the different focus depths of contrast curves in Figure 2(a). This indicates type C has low energy sensitivity and supports large process window which make it an ideal resist for grayscale process. Since both resists provide sufficient resolution for this step of work, type C was chosen for the following process development. The step height curve in Figure 2(a) shows the relationship between clearance depth and exposure dosage. The developed type C profile of 6 μm and 8 μm wide staircase patterns measured by profilometer is shown in Figure 2(b). The assigned dose for each step is 0.7, 0.5 and 0.4 of the averaged output energy measured around the write head. Since the resist depth is reduced 100 nm during development, the clearance depth contrast curve in Figure 2(a) was transferred nicely into the actual pattern profile in Figure 2(b). The vertical profiles of both stairs present similar amount of taper which is mainly determined by the light source wavelength. However, since 6 μm has shorter horizontal length, it results smaller step ratio (horizontal length / taper length between different step heights) in the profile. Following the same principle, it is harder to obtain large step ratio in smaller critical dimensions unless the step height is reduced either by reducing the total photoresist thickness or increasing the number of stairs.

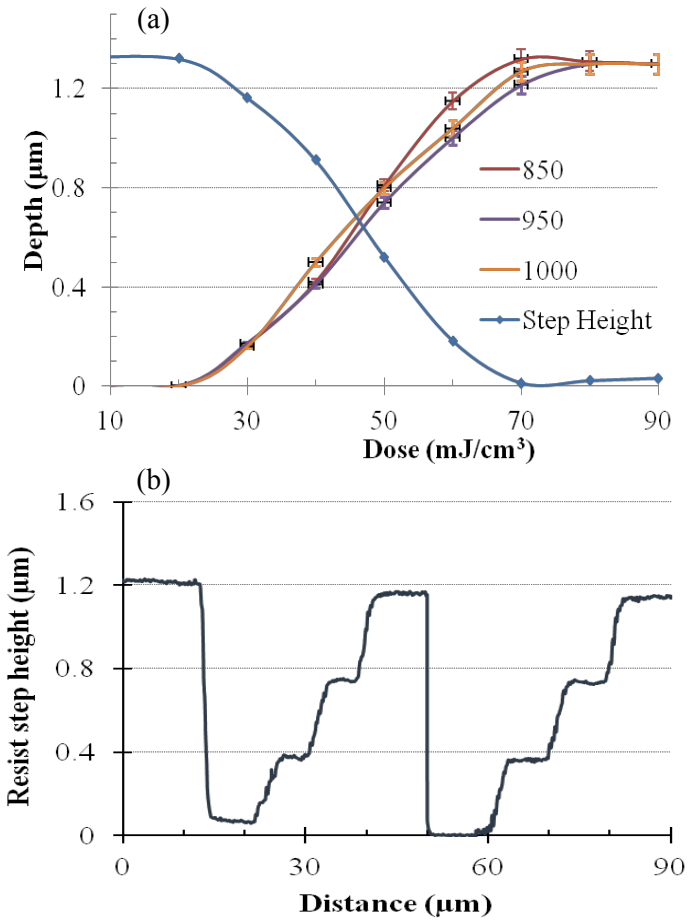

Figure 2. (a) The contrast curve of type C exposed by laser writer. This resist shows stable behavior over a wide range of focus depth, which are indicated in the legend in nm. The step height curve shows the relationship between clearance depth and dose. (b) The profile of 6 µm and 8 µm wide staircase pattern generated by laser writer.

Two types of substrates, SiO_2 and silicon, were patterned in order to generate two different topographies for process comparison. After the 1st lithography step, a developing time of 50 s was used and patterns were etched onto two substrates, a SiO_2 and silicon substrates. The deepest step in oxide film was etched down to 2 µm by RIE using O_2 and ChF_3 with a power of 200 W. This recipe gave 1:1.3 selectivity between oxide and photoresist and the result was confirmed using a profilometer. The silicon substrate was used to support deep etching in order to demonstrate the concept of integrating high topography substrate with grayscale structures written by e-beam. Grayscale patterned silicon wafer was etched down deeper than 30 µm by Inductively Coupled Plasma (ICP) etcher using the nanofab baseline recipe which contains Ar and SF_6 under radio frequency (RF) power 900 W with bias RF 12 W and backside He cooling. Etching monitor pads which are 150 µm wide, were included in the design to estimate the etching depth. The 1:6 aspect ratio of 0.7 µm stylus limits profilometer capability of profiling small features with deep topography. It is hard for the tip to reach deeper when the trench does not have sufficient wide opening.

The calibration of this stylus indicates the vertical accuracy of this method has error of about 3.2 % of the measured value on the 0.182 µm deep standard reference sample and error of 1.1 % of the measured value on the 0.971 µm deep standard reference sample.

2.2 Spray coating for e-beam grayscale lithography

To demonstrate the process of adding fine grayscale steps on high topography substrate, it is necessary to cover the planar and non-planar surfaces uniformly with reasonable e-beam resist thickness. Figure 3 shows the coating results on different topography substrates. Spin coating of 8 % volume fraction of 495 polymethylmethacrylate (PMMA) in anisole

provides uniform coverage over 2 μm deep topography through the entire pattern. However in the sample with 30 μm deep features spin coating fails to generate a usable film, as shown in Figure 3(b). The resist does not form a continuous layer especially around the sharp edges of deep trenches. The poor adhesion of resist to the sharp edges with large angles results in a graded structure where the resist is thinnest at the trench edge and gradually increases in thickness further away from the trench. It has been reported that spray coating is an ideal candidate for high topography structure in photolithography field.[7] It has only recently been applied to E-beam lithography field.[8,9]

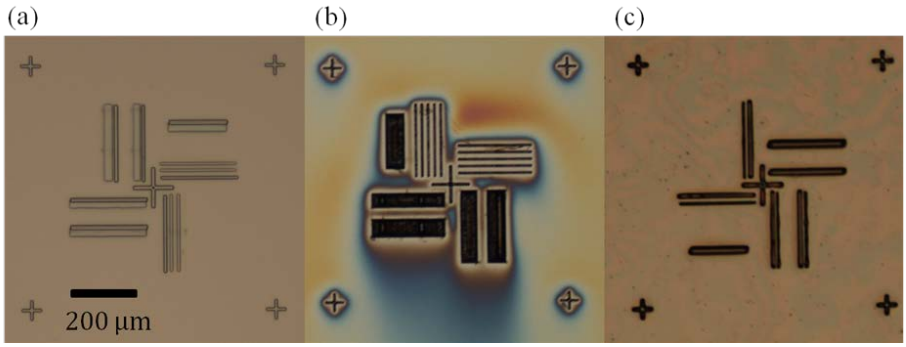

Figure 3. (a) Spin coating of PMMA on 2 μm deep staircase structure. It produces uniform film cross the pattern. (b)Spin coating of PMMA on 30 μm deep staircase structure. It presents poor coverage over the pattern area. (c) Spray coating of PMMA on 30 μm deep staircase structure. It produces nice coverage over the pattern.

Spray coating a 100 mm wafer with PMMA resist was performed with a tabletop spray coater. Atomic force microscopy (AFM) was used to collect the roughness of resist films and resist thickness was measured by profilometer. The spray coater was modified to use the Venturi effect to draw photoresist into the binary spay nozzle. The air pressure passing by the Venturi tube controlled the droplet size and flow rate of the photoresist. To optimize the spray coating process 100 mm diameter Si wafers were spray coated with varying parameters, such as dispensed volume and air pressure. In spray coating, the mixture of solvents provides a tradeoff between mobility of the spray resist droplets and solvent evaporation to prevent excessive flow of the resist. A crucial factor for spray coating of resist layers on samples with topography is the dilution ratio of the slow and fast evaporating components of the solvent mixture. However in our case with the vertical step, sidewall coverage is not regarded as critical as in the V-grove structure. This allows us to have increased flexibility on the resist selection. 4 % volume fraction of 495 PMMA in anisole was chosen in this work for its proper viscosity and a pressure of 86.18 kPa was found to produce the best result. A ≈5 mm wide single stripe (estimated by a digital caliper) with a thickness of ≈1.2 μm was generated under the stage moving speed ≈3 mm/s. The size of bubble defects increases with the spray flow rate. While using a low flow rate was observed to be helpful to obtain a uniform and thinner resist layer, the spray nozzle could no longer produce sufficient vacuum to draw in the PMMA below certain pressure threshold.

Following the spray coating, wafers were baked on a hotplate at 180 ^{o}C for 2 min. The roughness and uniformity of spray coated PMMA film is shown in Figure 4. Surface roughness is an important parameter for grayscale features since it is widely used in photonic device and the device efficiency is directly influenced by the surface roughness. For example, it needs to be less than 5 nm for gratings made for visible wavelengths. The spray coating film was measured to have average roughness (R_a) = 1.05 nm which is higher than spin coating film on the flat surface but still within the usable range. Profilometer was used to measure the film thickness after development over 13 clear lines distributed across the wafer center region as shown in Figure 4(c). The average thickness is 1.228 μm with a variation of +170 nm and -114 nm across the center 70 mm area of the wafer.

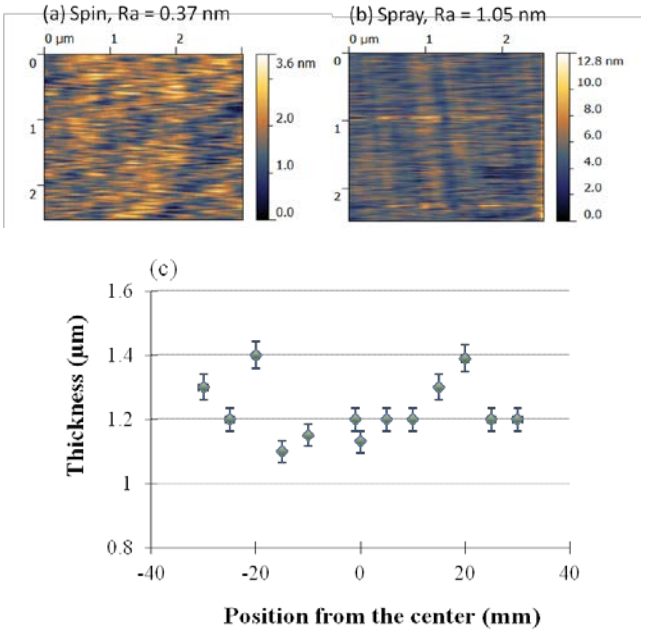

Figure 4. Roughness of PMMA film produced by (a) spin coating and (b) spin coating. (c) Thickness uniformity of spray coated PMMA across the wafer.

2.3 Grayscale e-beam lithography on high topography structure

The grayscale e-beam lithography was performed using electron beam writer with acceleration voltage 100 kV and beam current 0.20 nA. Atomic force microscopy (AFM) was used to collect resist profiles and microscopic structures were imaged by scanning electron microscopy (SEM). The uncertainties of AFM and SEM measurements were calibrated using SRMs dimension standard reference sample (RM8820). AFM measurements of the 97.3 nm ± 1.6 nm step feature on the reference sample indicate the AFM has the vertical precision of 0.9 nm ± 1.0 nm. This number is so small that the error bars in the measurement plots are smaller than the data marks. The uncertainties of SEM come from two sources, instrument built-in error and the user defined error. The instrument uncertainty of NanoFab SEM is less than 1 nm and the range of user defined error is estimated between 10 nm to 35 nm under the magnification of 15K.

The low sensitivity of PMMA makes it ideal candidate for grayscale lithography. Resist sensitivity is not as important since only a few components are fabricated and the low sensitivity makes the process more repeatable and controllable. In fact, the high sensitivity is not desirable because it makes the grayscale profile too sensitive to dose change and develop time. Keeping the resist height stable is important since a few tens of nanometer deviation of the profile can significantly change the optical properties of devices. In the wafers patterned by laser writer, 8 % PMMA in anisole was spin coated on the oxide wafer with 2 µm deep features and 4 % PMMA was applied by spray coating the 30 µm deep staircase silicon substrate. Three types of PMMA films were exposed by grayscale e-beam lithography in order to compare their grayscale performance. The resist conditions are listed in Table 2. Wafers were developed by volume ratio 1:2 H_2O/IPA (isopropyl alcohol) for 60 s. 1:2 H_2O/IPA was chosen in this study because it produces smaller resist roughness in PMMA film with thicknesses larger than 200 nm in comparison with the developers formulated by MIBK/IPA.[10]

Table 2. Conditions of three different PMMA films evaluated by grayscale e-beam lithography in this work. Spin coated 8 % PMMA was coated using 3000 min^{-1} and spin coated 4 % PMMA using 2000 min^{-1}.

PMMA in anisole	Thickness (nm)
Spin coated 8 %	≈440
Spray 4 %	≈1200
Spin coated 4 %	≈160

Figure 5 is the dose-depth profiles of three types of PMMA films. The figure indicates the spun on film of 4 % PMMA with 160 nm thickness has a relatively small grayscale dose range and high sensitivity compared with the other two films. This means it could only provide a limited grayscale levels and has a small process window. The concentrations of PMMA in the spin coated and spray coated films are the same so both films are supposed to have the same energy sensitivity which is represented by the slope of curve in the dose-depth profile. In Figure 5, these two curves do show the similar contrast slope with the increasing of dosages within the same thickness range. However, thinner resist requires much lower dose so its curve finishes in the very low energy domain, which makes the resist appear to be more energy sensitive. On the other hand, spin coated 8 % PMMA has lower sensitivity as indicated by the slope of contrast curve (red diamond marked line) in Figure 5. Based on the dose-depth profiles, a complex grayscale dose test array with 50 different dose combinations for the grayscale staircase pattern were exposed on 4 % spray coated PMMA and 8 % spin coated PMMA and the resulted resist profiles were evaluated by AFM. By analyzing this information, we are able to optimize the exposure conditions to certain level without the use of the proximity effect software simulation. This evaluation will be discussed in the next section. Two examples of grayscale patterns on two different PMMA films are shown in Figure 6. The patterns were exposed with the exposure base dose 350 μC/cm^2 with a 10 % increment up to 700 μC/cm^2. The deepest step was not fully profiled due to the limitation of AFM tip shape and the vertical loading angle. The grayscale patterns on high topography substrates are shown in Figure 7.

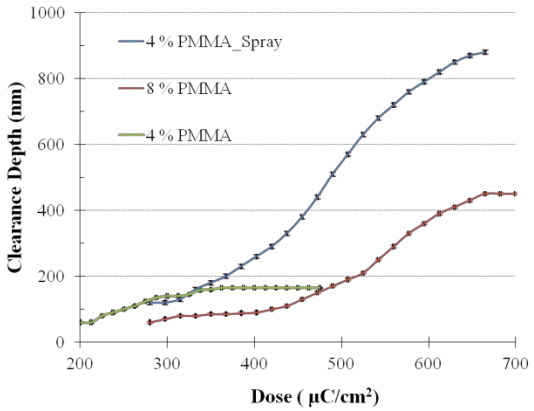

Figure 5. The dose-depth profiles of three types of PMMA films prepared for grayscale e-beam lithography. The error bars are overlapped with data marks.

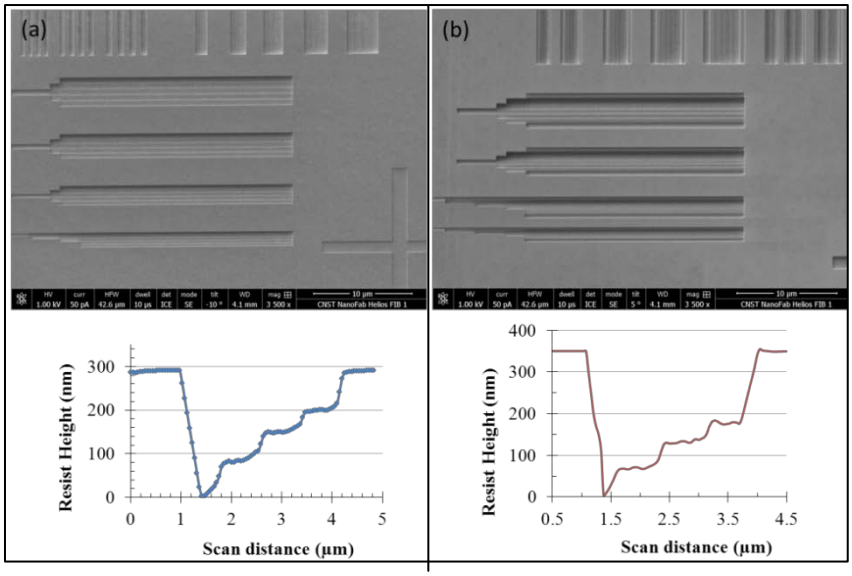

Figure 6. SEM and AFM cross section results of grayscale pattern on flat surface using (a) spin coated 8 % PMMA (b) spray coated 4 % PMMA. The bottom row is the AFM cross section profile of the patterns shown in SEM image.

3. DISCUSSION

3.1 Alignment strategy

Different from the conventional two global alignment marks strategy, a set of e-beam global alignment marks corresponding to different step heights in the pattern was exposed by a laser writer in the 1st lithography step. Due to the high topography substrate structure, this design provides a focal plane for the electron beam at each depth to maintain the sharpness of the beam (resolution). Note it may not be required in each step height, depending on the convergence angle (depth of field) of the beam in the lithography tool.

The final grayscale patterns, the combined results of two different lithography steps, are shown in Figure 7. The shallow topography on the oxide sample is shown in Figure 7(a) and the deep topography on the silicon substrate is shown in Figure 7(c). The focus and alignment strategy was successfully applied and the fine e-beam grayscale patterns were placed in each step height as designed to create the fine grayscale patterns over a large depth range. In 2 μm deep case, the initial alignment error was estimated to be 115 nm which is much larger than the capability of this E-beam lithography system. However, much of this error is due to the etching bias. After the width broadening caused by etching process was taken into account, alignment accuracy better than 100 nm was achieved. In the 30 μm deep substrate case, it is not applicable to use the same correction method due to the large edge roughness caused by deep silicon etching. Figure 7(d) shows a 159 nm roughness at the edge between the surface level and the deepest level, 30 μm. This makes the estimation of overlay error hard to define so we do not quote one for the silicon substrate.

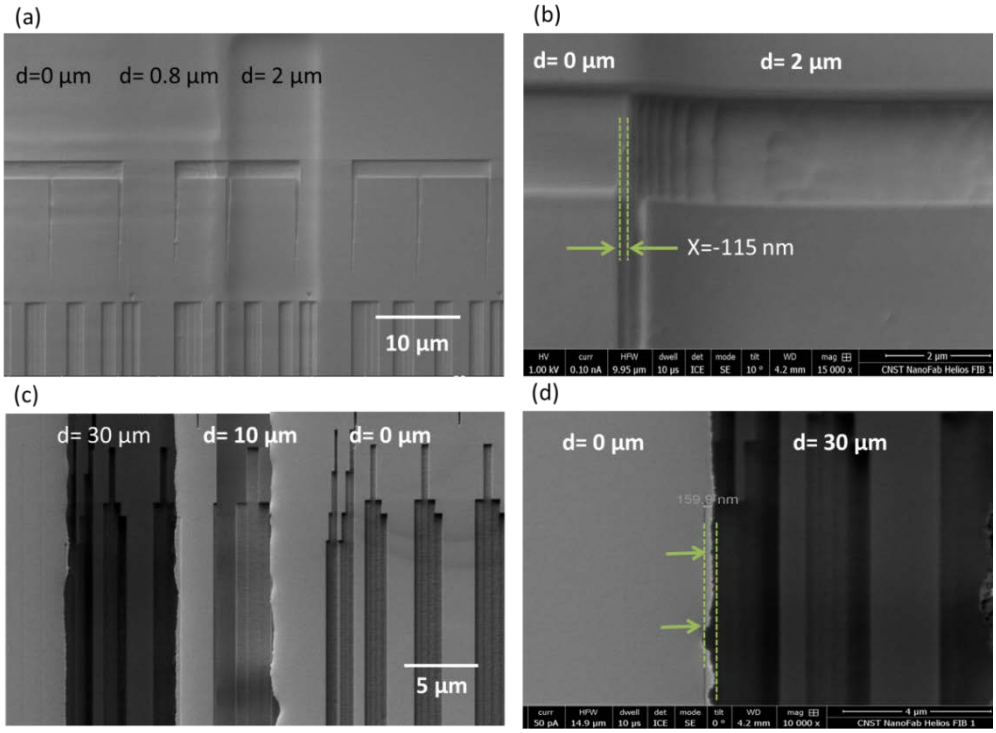

Figure 7. The final grayscale patterns on oxide and silicon substrates with different topographies. (a) E-beam written stair pattern on 2 μm deep substrate. (b) The overlay evaluation pattern indicates 115 nm overlay error. (c) E-beam written stair pattern on 30 μm deep substrate. (d) The large edge roughness makes it hard to estimate the overlay error and improve the overlay.

3.2 Proximity effect limitation

Proximity correction is necessary in e-beam lithography to account for the forward and backward electron scattering and the secondary effects it causes. The proximity correction introduces additional complexity into the design process. In all of these methods, the first step in grayscale profile design is always to generate the spatial dose profile of the features. This step includes the dose-depth curve from experimental data and the spatial depth profile of the grayscale feature. The spatial dose profile can then be used in a proximity correction algorithm to output a modified spatial dose profile. A double-Gaussian function as shown in equation (4) is used to approximate the point-spread function.

$$f(r) = \frac{1}{\pi(1+\delta)}\left(\frac{1}{\eta^2}e^{-r^2/\eta^2} + \frac{\delta}{\beta^2}e^{-r^2/\beta^2}\right). \quad (4)$$

where η is the forward scattering parameter, β is the backscatter parameter, δ is the ratio of the backscattered to forward scattered energies, and $r = \sqrt{x^2 + y^2}$ is the radial distance. The point spread function contains the important information about the energy spread in the spatial range. By adding the point spread function at each pixel together the total energy distribution of a certain design could be estimated and adjusted according to the dose-depth profile. This effective dose-depth method[10] is probably one of the simplest proximity correction methods. The proximity effect correction in grayscale has significant impact in the practical design when a certain slope, shape and grayscale dimensions need to be achieved. The main purpose of this paper is trying to explore the resolution of grayscale lithography using basic pattern shape and compare different topography and resist performance in a relative manner. The proximity effect in each design mutually cancelled out so this correction will not produce significant difference on the comparison result. Alternatively, the spatial depth profile of the grayscale feature could be estimated experimentally by AFM measurements on grayscale dose test array which contains systematic designed different dosage combinations and corrected by manual pattern fracturing. Although it is not able to perform pixel by pixel correction, it provides sufficient data for dose correction on 100 nm scale patterns as shown below compared with other literatures with simulated proximity effect correction.

Regarding the staircase pattern we used in this paper, the relationship between grayscale vertical resolution and horizontal critical dimension (CD) in PMMA resist with different thicknesses is summarized in Figure 8. This resolution-CD relationship is very similar in both types of PMMA films we evaluated in Figure 6 at the same clearance depth. A step height around 30 nm is achievable in the larger CDs and the minimum step height increases with the decreased CD as the effects of forward scattering grow. It was also found that the thicker film has worse resolution than a thinner film with the same level of step height. In many practical cases it is useful to have the resist clear at the darkest grayscale level. Here that would require adding more steps or increasing the step height. However there is also an aspect ratio limitation on the step height versus CD. While the step height in 4 % PMMA spray coated film was increased to 200 nm in 600 nm CD pattern, the taper length also increased to be equal to the CD length. The step ratio decreases to 1 in this case and it started to lose the step profile. The increasing of step height causes the increasing level of resist tapering and eventually the resist profile loses definition and turns to be a continuous slope rather than a series of steps which is desirable in some grayscale applications.

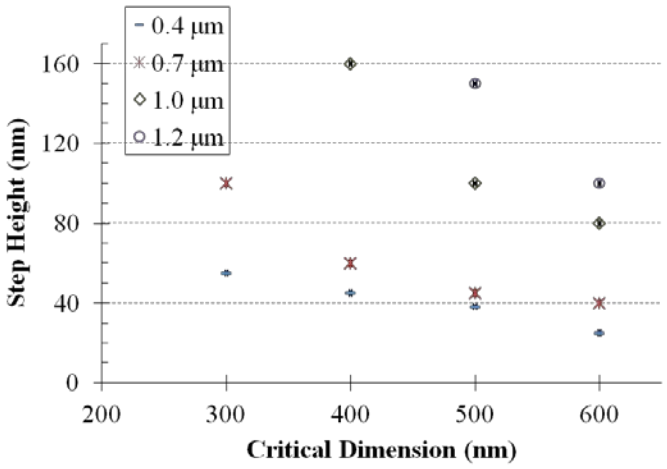

Figure 8. The relationship between grayscale vertical resolution and horizontal CD from 4 steps staircase pattern in spray coated PMMA films with different clearance depth. AFM measurements error is estimated to be around 1.0 nm using standard reference sample so the error bars are overlapped with the data marks.

4. CONCLUSION

The combination optical and electron beam lithography techniques to produce grayscale lithography of the nano-scale was demonstrated using the design of nano-scale staircase pattern on the micro-scale staircase pattern. With a proper

alignment strategy and spray coating of e-beam resist, the fine e-beam grayscale staircase patterns were successfully placed on high topography substrate with 30 μm deep steps. The vertical resolution achieved is measured to be 25 ± 5 nm in 600 nm CD and 45 ± 6 nm in 300 nm CD using two different types of PMMA films. The aspect ratio limitation between step height and CD is observed especially in the thick resist. A complementary lithography overlay error smaller than 100 nm was achieved in the shallow topography case. The large edge roughness from deep silicon etching makes the overlay error difficult to be estimate in the 30 μm case and further edge smoother process is required in the high overlay requirement application.

ACKNOWLEDGEMENT

Authors would like to thank Mr. Matt Robison for his assistance on profilometer data collection. We sincerely appreciate Dr. Kerry Siebein for the valuable discussion on the measurement uncertainty analysis.

REFERENCES

[1] Y. Opplinger, P. Sixt, J. M. Stauffer, J. M. Mayor, P. Regnault, and G. Voirin, “One-step 3D shaping using a gray-tone mask for optical and microelectronic applications,” Microelectron. Eng., 23, 449–454 (1994).

[2] Chuck Che-Kuang Wu, "Gray Scale All Glass Photomasks," U.S. Patent No. 6,524,756, Feb. 25 2003.

[3] G. Gal, “Method for fabricating microlenses,” U.S. Patent No. 5,310,623, 10, 1994.

[4] M. Ekberg, F. Nikolajeff, M. Larsson, and S. Hard, “Proximity-compensated blazed transmission grating manufacture with direct-writing, electron beam lithography,” Appl. Opt. 33, 103 (1994).

[5] Borodovsky, Y., “MPProcessing for MPProcessors,” SEMATECH Maskless Lithography and Multibeam Mask Writer Workshop, May 2010.

[6] David K. Lam, Enden D. Liu, Michael C. Smayling, Ted Prescop, “E-beam to complement optical lithography for 1D layouts,” Proc. SPIE, 797011 (2011).

[7] Nga P Pham, Joachim N Burghartz and Pasqualina M Sarro, “Spray coating of photoresist for pattern transfer on high topography surfaces,” J. Micromech. Microeng. 15, 691–697 (2005).

[8] J. Linden, Ch. Thanner, B. Schaaf, S. Wolff, B. Lägel, E. Oesterschulze, “Spray coating of PMMA for pattern transfer via electron beam lithography on surfaces with high topography,” Microelectron. Eng., 88, 2030–2032 (2011).

[9] Siddarth Srinivasan, Shreerang S. Chhatre, Joseph M. Mabry, Robert E. Cohen, Gareth H. McKinley, “Solution spraying of poly(methyl methacrylate) blends to fabricate microtextured, superoleophobic surfaces,” Polymer, 52, 14, 3209-3218 (2011).

[10] Raghunath Murali, Devin K. Brown, Kevin P. Martin, and James D. Meindl, “Process optimization and proximity effect correction for gray scale e-beam lithography,” J. Vac. Sci. Technol. B 24, 2936 (2006).